

## AGGLOMERATE DISPERSION IN CAVITATING FLOWS

J. Baldyga<sup>a\*</sup>, Ł. Makowski<sup>a</sup>, W. Orciuch<sup>a</sup>, C. Sauter<sup>b</sup>, H.P. Schuchmann<sup>b</sup>

<sup>a</sup> Faculty of Chemical and Process Engineering, Warsaw University of Technology,  
ul. Waryńskiego 1, 00-645 Warsaw, Poland; e-mail: [baldyga@ichip.pw.edu.pl](mailto:baldyga@ichip.pw.edu.pl)

<sup>b</sup> University of Karlsruhe, Institute of Engineering in Life Science, Food Process  
Engineering, Kaiserstrasse 12, 76128 Karlsruhe, Germany

**Abstract.** For a long time, erosion induced by cavitation has been an important technological and research problem in the fields utilizing fluid-handling machinery [1, 2]. The air/vapor bubbles are nucleated in a region where the pressure is sufficiently small, they grow and possibly form cavities, and are transported to regions of higher pressure where the bubbles collapse, creating locally high stresses and perhaps damaging apparatus surfaces. The same mechanism can cause breakage of agglomerates suspended in the liquid, when the suspension flows through the micro-nozzle to induce very high hydrodynamic dispersing stresses. In this paper we investigate experimentally and numerically the flows through the nozzles of diameter between 80  $\mu\text{m}$  and 200  $\mu\text{m}$  under pressure difference up to 2400 bar. Experiments are performed for fumed silica Aerosil 200V agglomerates. The cavitation model is used with the mixture multiphase model and k- $\epsilon$  CFD code by FLUENT. The CFD model is implemented with the population balance for agglomerates and rheological equations for aggregated suspension, and applied to simulate the process and interpret experimental data.

**Key words:** Agglomerates, Aggregates, Deagglomeration, Cavitation, High pressure nozzle;

### 1. INTRODUCTION

Suspensions consisting of nanoparticles and nanoparticle clusters are applied to formulate numerous products of practical importance. To manufacture such suspensions one needs to incorporate nanoparticles in the liquid phase, disintegrate nanoparticle clusters and finally stabilize the suspension. Very often at first a pre-dispersion is produced in a device characterized by lower shear and afterwards the desired suspension is formulated in the high shear device. In our previous publications [3, 4] we presented the findings of both numerical and experimental study on dispersing nanoparticle clusters using an in-line rotor stator and the ultrasonic device. In this paper, the findings of experimental and numerical studies will be presented for the high pressure nozzle dispersing system. Some preliminary simulation results for the high-pressure device we have published previously [5, 6]; here we present the complete model, compare model predictions with experimental data, and discuss in this context different methods of modeling.

To disperse agglomerates in the high-pressure nozzle device, the high pressure difference between the capillary inlet and outlet is applied to cause high velocity flow through the capillary and induce this way the high hydrodynamic stresses. The hydrodynamic stresses have different character depending on position in the system: at first the fluid elements entering the nozzle are significantly accelerated, which means that there are strong stresses

resulting from elongation of fluid elements; when the suspension is flowing through the nozzle the flow is weakly turbulent with the pipe Reynolds number equal roughly to 4000, so there are viscous and inertial turbulent stresses, and finally when the suspension leaves the nozzle, a turbulent jet is formed and high hydrodynamic stresses are created. However, the flow is more complex than presented above and this is due to cavitation phenomena. Namely, at high velocity regions the pressure becomes very low and cavitation bubbles consisting of desorbed air and water vapor are nucleated. Cavitation occurs when the pressure falls sufficiently low, which can be characterized by the cavitation number:

$$CN = \frac{p - p_v(T)}{\frac{1}{2} \rho_L U_\infty^2} \quad (1)$$

where  $p_v(T)$  is a saturated vapor pressure,  $\rho_L$  represents liquid density, and  $U_\infty$  is a reference velocity. Cavitation occurs when CN is reduced below a limiting value called incipient cavitation number [2]. Afterwards the bubbles grow and either they are conveyed to regions of higher pressure, or the flow may involve separation, and a cavity may be formed. In the second case the bubbles may be created by entrainment by the turbulent liquid from the cavity interface. In either case when they are transported by the flow to the higher pressure region downstream where the liquid flow reattaches to the wall, they can collapse in close proximity of the wall and possibly damage it locally [1]. Collapse of cavitation bubble can create very high local pressures and velocities; the high velocity microjets have for example the velocity about 300 m/s and diameter between 1 $\mu$ m and 10  $\mu$ m [1]; moreover the same time the shock waves are induced. Both microjets and shock waves depict a local release of energy at an enormous rate, which can cause material damage. Erosion induced by cavitation has been since many years an important technological and research problem in the fields utilizing fluid-handling machinery and much of the past research was on cavitation damage [1, 2]. In the case of aggregated suspension collapse of bubbles in the proximity of nanoparticle clusters may break them into pieces. Cavitation should be thus considered as a contributory mechanism for deagglomeration.

Another effect of cavitation to be considered in what follows is a change of the flow pattern resulting from presence of bubbles. The multiphase nature of the high Reynolds number flow with large differences in properties of each phase makes the problem difficult. A common approach in modeling cavitation flow is to use the relatively simple mixture multiphase models that are based on transport equations for either mass or volume fraction of considered phases. Then the main problem is related to proper definition of the evaporation and condensation terms. Interesting comparison of three different recently proposed models is given in [7]; in this publication the work is motivated by the fact that “there is a lack of clear consensus of the capability and relative merits” of the considered approaches. The conclusion is that all three models predict well the wall pressure distribution but they are handling differently compressibility effects, and the further research is needed to address some modeling uncertainties. The authors [7] have found merits and limitations in all considered models. Anyhow we will use one of them [8] to model cavitating flows but should remember that there can be some error in predicted results. A model material for investigation of agglomerate disintegration in high-pressure nozzle in this work is the hydrophilic fumed silica manufactured by Degussa and called Aerosil 200V.

## 2. EXPERIMENTAL

The process of dispersion of nanoparticle clusters (Aerosil 200V by Degussa) in high-pressure nozzle device was investigated experimentally in the laboratory of Institute of Engineering

Life Sciences, Food Process Engineering of University of Karlsruhe. Investigations were carried out for the solid content in a range between 1wt.% and 12.5 wt.%. Before carrying out dispersion experiments the pre-dispersions were prepared by mixing the appropriate amount of Aerosil powder with demineralised water in a stirred tank equipped with a paddle impeller. Pre-dispersion preparation time was constant for each particle concentration and equal to 15 minutes. The zeta potential of Aerosil was measured by using ultrasound spectroscopy (AcoustoSizer II, Colloidal Dynamics); it was above -30 mV, which means that there is some electrostatic repulsion stabilizing the suspension. It is well known that agglomeration of silica is more affected by chemical effects than repulsion [9]. For example at pH close to 2, so near silica zero charge point, silica sols are stable. On the other hand agglomeration effects are observed above pH 7.3. However, not discussing more about mechanism and conditions promoting agglomeration it was checked experimentally that all dispersions considered in this work were stable for weeks.

For high pressure dispersing experiments an apparatus presented schematically on Fig.1 was applied. The configuration consisted of a vessel, supplying demineralised water, a high pressure pump, a coiled tube and the nozzle fitting.

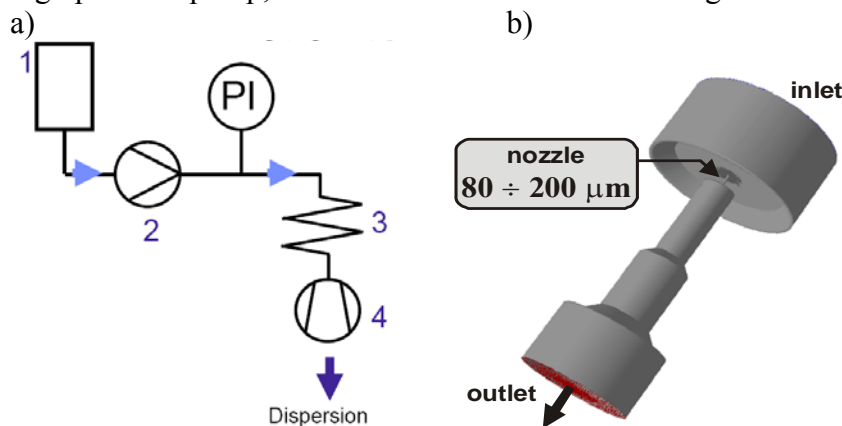


Fig. 1. a) Schematic of high-pressure set-up: 1. a water reservoir, 2. a high pressure pump, 3. a coiled tube, 4. A nozzle fitting b) a nozzle represented by CFD hexahedral mesh (577 810 cells, 599 140 nodes)

The pressure level was adjusted (up to 3000 bar) using demineralised water and afterwards the fitting was removed, the pre-dispersion introduced into the coiled tube, and the nozzle installed again. The coiled tube was applied as reservoir for the suspension with a capacity of 140 cm<sup>3</sup>. Using this method the suspension was not entering the high pressure pump. In experiments the nozzles of diameter between 80 μm and 200 μm were applied. The suspension leaving the nozzle was collected in a vessel and the size of particles and aggregates measured by 90° photon correlation spectroscopy (Coulter N4, Beckmann Coulter) and laser diffraction combined with Polarization Intensity Differential scattering technology (PIDS, LS 230, Beckmann Coulter), the latter to control modality of PSD. In similar way the pre-dispersion PSD was measured. Experimental data will be shown in Section 4 of this paper together with model predictions.

### 3. MODEL PRESENTATION

Aerosil fumed silica particles have a cluster-fractal structure [10, 11]. The large agglomerates of a size  $L_i$  (10- 200μm) consist of smaller primary aggregates of a size  $L_a$  (100–500 nm), which are composed of primary silica particles of a size  $L_0$  (5 nm–50 nm) [12]. The primary particles are connected by strong chemical bonds (hydrogen and siloxane bonds) forming strong aggregates. The aggregates forming agglomerates of size  $L_i$  are connected by adhesion forces and thus agglomerates are less stable than aggregates. They can be disintegrated by stresses resulting from hydrodynamic effects. Their mass is related to the size by the fractal

geometry [3]. Fractal geometry is also used to estimate the tensile strength of agglomerates. The number of bonds connecting aggregates in an agglomerate can be related to the agglomerate porosity by following equation [13, 14]:

$$\sigma_T = 1.1 \frac{1 - \varepsilon_a}{\varepsilon_a} \frac{F}{L_a^2} = -1.1 \frac{1 - \varepsilon_a}{\varepsilon_a} \frac{HaR_0}{24H^2L_a^2} \quad (2)$$

where  $F$  represents the bonding force between aggregates in the agglomerate that is calculated using the classical DLVO theory; in present case  $F$  is expressed by the van der Waals forces calculated assuming that all primary particles have equal radii,  $R_0$ :

For the porosity  $\varepsilon_a$  one can use either the average agglomerate porosity,  $\bar{\varepsilon}_a$ , when the dominating dispersion mechanism is breakage, or the “external porosity” ,  $\varepsilon_a(L)$  when erosion dominates dispersion, as described in [3, 4]. Both porosities are calculated using fractal geometry. The main qualitative difference between the mechanisms of rupture and erosion is energy input [15, 16]. It is low for erosion and high for rupture and shattering. More precisely this is represented by the fragmentation number defined in [15, 16]; for the stress  $\tau$  and it can be expressed by [4]:

$$Fa = \frac{24\tau\varepsilon_a L_a^2 H^2}{1.1(1 - \varepsilon_a) HaR_0} \quad (3)$$

In the case of the rotor-stator device, at least under experimental conditions applied in [3], erosion has been identified as the dominant Aerosil dispersion mechanism. In the case of high-pressure device considered in this work the stresses are locally much higher than that induced in the rotor-stator, so also rupture type dispersion is possible. The stresses are generated due to the flow and in what follows we consider hydrodynamic stresses and stresses induced by cavitation. The hydrodynamic stresses can be expressed using local values of the rate of energy dissipation  $\varepsilon$ :  $\tau = \mu (\varepsilon/\nu)^{1/2}$  for agglomerates smaller than the Kolmogorov microscale,  $\lambda_K = \nu^{3/4} / \varepsilon^{1/4}$ , and  $\tau = \rho \varepsilon^{2/3} L_i^{2/3}$  for  $L_i > \lambda_K$ . The stresses generated by bubble implosion can be estimated using the semiempirical equation [17].

$$\tau_p = \alpha \rho_L c V_j \quad (4)$$

where  $c$  is the velocity of compressional wave in the liquid,  $V_j$  is the microjet velocity and  $\alpha$  is a constant that varies from 0.41 to 3.0. In what follows we use  $\alpha = 2$ . The microjet velocity is estimated as a ratio of the bubble radius and the total Rayleigh collapse time [2],

$$V_j = \frac{R_0}{t_{tc}} = \frac{(p - p_v)^{1/2}}{0.915 \rho_L^{1/2}} \quad (6)$$

For stresses higher than the tensile strength of agglomerates, agglomerates smaller than the Kolmogorov microscale break up with the frequency  $\Gamma_h = C_b (\varepsilon/\nu)^{1/2}$  and those larger with  $\Gamma_h = C_b (\varepsilon L_i)^{2/3}$ . This defines the breakage kernel,  $\Gamma_h$  with  $C_b$  being a proportionality constant that should be fitted to experimental data.

The frequency of breakage induced by cavitation is estimated using Fluent, where the cavitation source terms are defined using the Singhal model [8].

$$R_C = C_C \frac{\sqrt{k}}{\sigma} \rho_L \rho_L \sqrt{\frac{2(p - p_v)}{3\rho_L}} m_v \quad \text{for } p > p_v \quad (7)$$

In the expression for the vapor condensation rate  $R_c$ ,  $m_V$  is the vapor mass fraction,  $k$ , kinetic energy of turbulence,  $\sigma$  denotes interfacial tension, and  $C_C$  is an empirical constant. In computations  $C_C = 0.01$  is used as recommended by Fluent. The rate of collapse of bubbles is defined as a ratio of mass condensation rate to the mass of a bubble:

$$\Gamma_c = C_{bc} \frac{R_c}{\frac{4}{3} \pi R_0^3 \rho_V} \quad (8)$$

with  $C_{bc}$  being empirical constant. The bubble radius value,  $R_0$ , is expressed using the Blake equation for the critical bubble diameter [2],  $d_{crit} = 8\sigma / [3(p_V - p)]$ . In dispersion simulations a superposition of both dispersion mechanisms was assumed, yielding for the breakage kernel

$$\Gamma(L) = \Gamma_h(L) + \Gamma_c(L) \quad (9)$$

Due to action of shear and breakage there is variation of the agglomerate structure that can be expressed [3] by evolution of the fractal dimension  $D_f$  and interpreted as a superposition of relaxation effects: compressing with the driving force proportional to  $3 - D_f$ , and breakage with its limiting value defined by mass and volume conservation.

$$\frac{D D_f}{D t} = G_{D_f} = C_{shear} \dot{\gamma} (3 - D_f) + C_{break} \Gamma (D_{f, break(min)} - D_f) \quad (10)$$

The above equations for breakage and restructuring are introduced to the population balance equation; in what follows the moment transformation of the population balance equation together with the quadrature method of moments (QMOM) [18] are used,

$$\frac{\partial m_k(\bar{x}, t)}{\partial t} + u_i \frac{\partial m_k(\bar{x}, t)}{\partial x_i} = \frac{\partial}{\partial x_i} \left[ D_r \frac{\partial m_k(\bar{x}, t)}{\partial x_i} \right] + \sum_{i=1}^n \Gamma_i b_i^{(k)} w_i - \sum_{i=1}^n L_i^k \Gamma_i w_i - \frac{1}{D_f} G_{D_f} k \sum_{i=1}^n L_i^k w_i \ln \left( \frac{L_i}{L_a} \right) \quad (11)$$

where  $b_i^{(k)}$  is given by  $b_i^{(k)} = 2^{1 - \frac{k}{D_f}} L_i^k$  for rupture and  $b_i^{(k)} = N L_a^k + (L_i^{D_f} - N L_a^{D_f})^{k/D_f}$  for erosion, with number of fragments  $N$  being a function of agglomerate geometry [3]. In computations  $n=3$  Dirac delta impulses with  $2n=6$  moments are used to simulate features of the complete distribution (i.e. yielding the same moments). The last term on the r.h.s of eq.(11) describes variation of agglomerate size due to restructuring. The population balance equations and the mixture multiphase model equations are connected to the  $k$ - $\epsilon$  CFD code by FLUENT and used to simulate the flow and disintegration processes. The mixture density and viscosity are calculated based on local volume fractions of suspension, vapor and air. The continuity and momentum balance equations are solved for the mixture, and the additional balance equation for the gaseous phase is used. In computations the effective viscosity of the suspension is applied to define the liquid phase viscosity that is applied in the mixture multiphase model. The suspension viscosity is calculated based on the Buyevich and Kabpsov model [19] in a form applicable for fractal agglomerates [3]; the effective viscosity depends in this model on the effective volume fraction of agglomerates and agglomerate size distribution.

Results of simulations presented in next section of this paper were obtained for following Aerosil and process parameters:  $L_a = 150$  nm, initial value of  $D_f$  equal to 2.85, agglomerate strength characterised by  $Ha = 5 \cdot 10^{-21}$  J,  $H = 10^{-9}$  m, and for breakage constant  $C_b = 2 \cdot 10^{-3}$  [3]. The  $C_{bc}$  values used in computations are equal to  $2 \cdot 10^{-16}$  and  $2 \cdot 10^{-18}$  for the rupture and erosion respectively. The pre-dispersion fed into the nozzle was characterized by measured PSD; it was a unimodal distribution of agglomerate size with  $L_{10} = 8.8$   $\mu\text{m}$ ,  $L_{20} = 11.8$   $\mu\text{m}$ ,  $L_{30} = 15.7$   $\mu\text{m}$ ,  $L_{32} = 29.6$   $\mu\text{m}$ .

#### 4. RESULTS, DISCUSSION AND CONCLUSIONS

Figure 2 shows simulated distributions of the volume fraction of the gas phase  $f_g$  (comprising of the vapor and air) in the system. The cavities are formed close to the nozzle outlet in both geometries (80 and 200  $\mu\text{m}$ ) and different values of pressure drop. They are followed by a region of decreasing volume fraction of the gas phase, where the bubbles are collapsing and cavitation stresses are created. Extent of the cavity is larger for larger nozzle diameter.

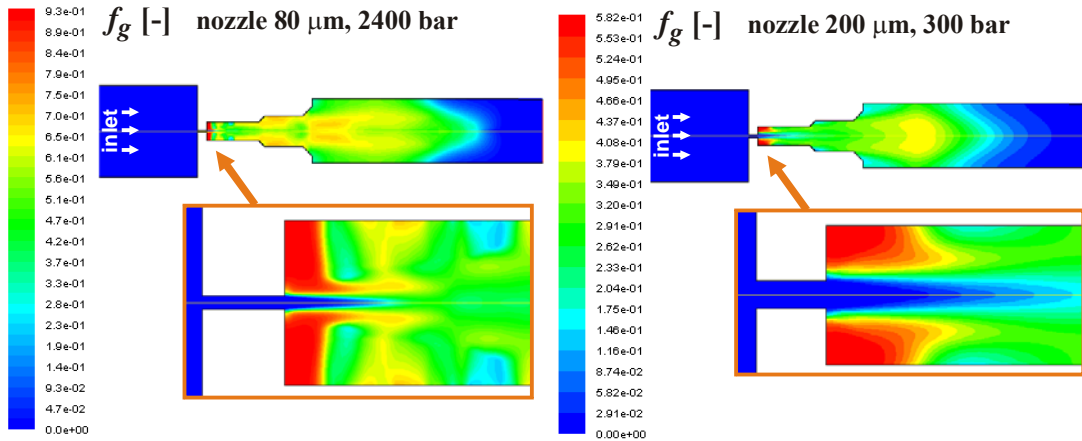


Fig. 2. Distribution of the gas phase volume fraction in two high-pressure devices.

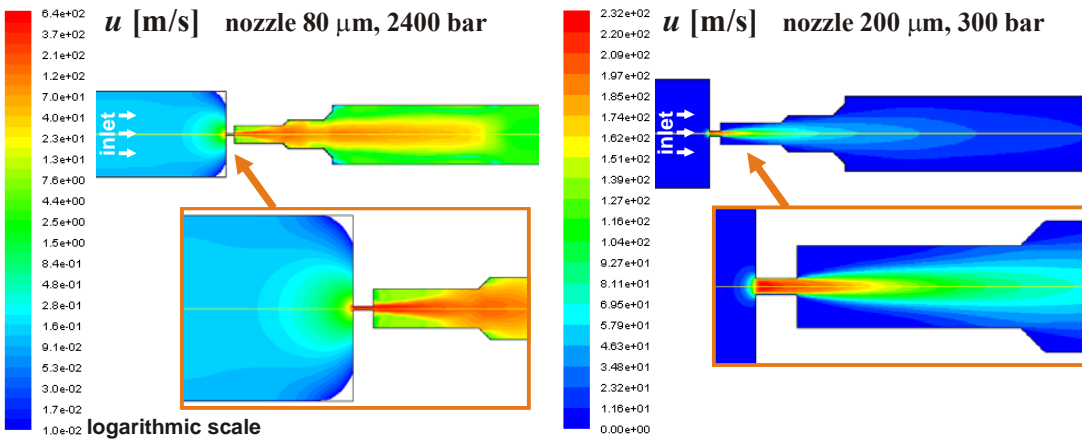


Fig. 3. Velocity distribution of the gas phase volume fraction in two high-pressure devices.

Figure 3 shows the velocity distribution for the same flows. Here one can see that for the small, 80  $\mu\text{m}$  nozzle, there is very high increase of the velocity, high acceleration and very high hydrodynamic stresses created in fluids entering the nozzle. Very high velocities induced in the nozzle and the jet result from very high pressure drop, and they create very high turbulent stresses.

Effects of hydrodynamics and cavitation induced stresses on dispersion are compared on Fig.4, where the breakage kernel values for agglomerates of the size 8.8 $\mu\text{m}$  are presented for the 80 $\mu\text{m}$  nozzle. One can see that the hydrodynamic stresses are acting already at nozzle entrance, afterwards within the nozzle and finally in the jet, whereas the stresses induced by cavitation become effective later, in the jet, where the bubble collapse. Figure 5 shows where actually disintegration takes place, and most of disintegration is in a jet. There is also some increase of the fractal dimension observed in this case, which results from action of stresses.

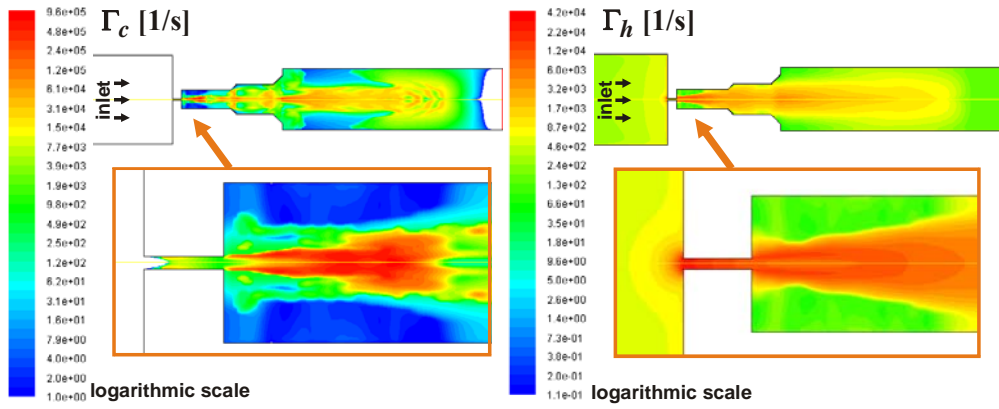


Fig. 4. Breakage kernel distribution in the 80µm nozzle high-pressure device.

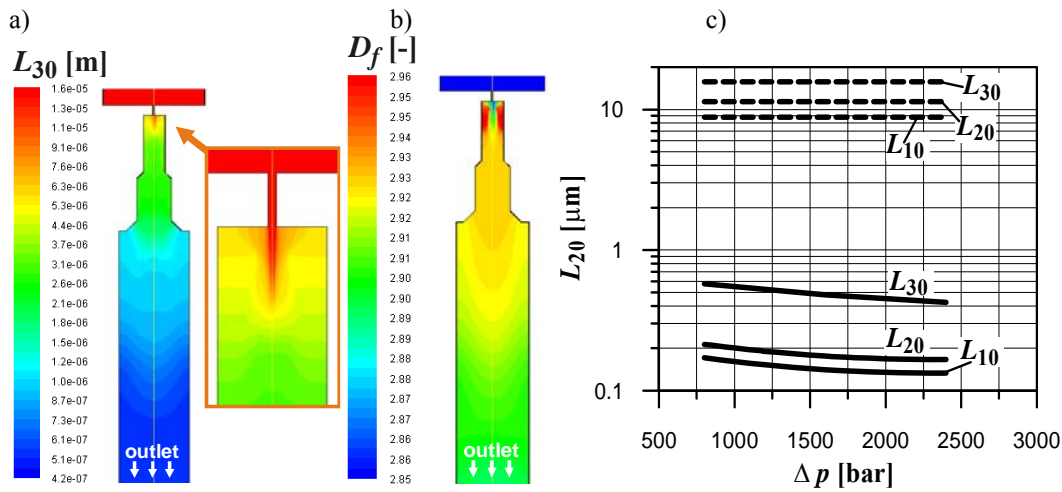


Fig. 5. Results of computations: a) agglomerate size distribution b) fractal dimension distribution, c) predicted effect of pressure drop on agglomerate size for the 80µm nozzle (rupture mechanism of dispersion).

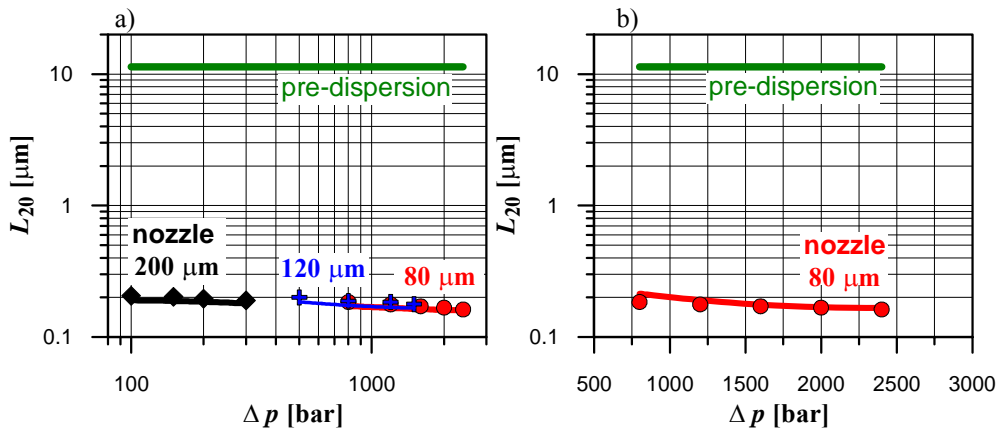


Fig. 6. Comparison of model predictions with experimental data: a) based on erosion mechanism b) based on rupture mechanism. Experimental results are marked by points, and lines represent results of simulations.

Finally it is shown that effect of disintegration for just one passage through the device is very large, much larger than in the case of the rotor-stator [3, 5]. Figure 6 shows comparison of model predictions with experimental data. It can be seen that a good agreement is observed for both mechanisms, erosion and rupture. This is done by fitting the constant  $C_{bc}$  to experimental data. Using just experimental agglomerate size distributions we cannot judge which mechanism is more active as this was possible when the rotor-stator data were interpreted with bimodal distribution clearly observed. Here the process of disintegration is so advanced that we observe just initial and final unimodal distributions. Based on the value of

the fragmentation number, several orders of magnitude larger than in the case of rotor-stator, we suppose that the rapture, or possibly shattering, represent mechanism that dominates disintegration of Aerosil agglomerates in the high-pressure device under considered process conditions. One can also conclude that the method based on combining the CFD approach with population balancing and including effects of agglomerate and suspension structure on suspension viscosity leads to reasonable results that are confirmed by experimental data.

## 5. REFERENCES

1. Hammit F.G., 1980. *Cavitation and Multiphase Flow Phenomena*. McGraw-Hill, New York.
2. Brennen, C.E., 2005. *Fundamentals of Multiphase Flow*. Cambridge University Press, New York.
3. Bałdyga, J., Orciuch, W., Makowski, Ł., Malik, K., Ozcan-Taskin, G., Eagels W., Padron, G., 2008. “Dispersion of nanoparticle clusters in a rotor-stator mixer”, *Ind.Eng. Chem. Res.*, **47**, 3652-3663.
4. Bałdyga, J., Orciuch, W., Makowski, Ł., Sauter C., Schuchmann H.P., “Deagglomeration processes in high shear devices” 2008. Submitted to *Chem. Eng. Res., Des.*,
5. Bałdyga, J., Orciuch, W., Makowski, Ł., Malski-Brodzicki M., Malik, K., 2007. “Break up of nano-particle cluster in high-shear devices”, *Chem. Eng. Process.* **46(9)**, 851-861.
6. Bałdyga, J., Orciuch, W., Makowski, Ł., Krasinski, A., Malski-Brodzicki, M., Malik, K., 2008,.”Shear flow of aggregated nanosuspensions-fundamentals and model formulation” *Journal. Disp. Sci. Tech.*, **29**, 564-572.
7. Senocak I., Shyy W., 2002. “Evaluation of cavitation models for Navier-stokes Computations” *Proceeding of FEDSM’02, 2002ASME Fluids Engineering Division Summer Meeting*, Montreal, Quebec, Canada, July 14-18, FEDSM2002 – 31011.
8. Singhal A.K., Athavale M.M., Li H., Jiang Y, 2002. “Mathematical Basis and Validation of the Full Cavitation Model”, *Journal Fluids Eng.*, **124**, 617-624.
9. Depasse, J., 1999. “Simple experiments to emphasize the main characteristics if the coagulation of silica hydrosols by alkaline cations: application to the analysis of the model of Colic et al.” *Journal of Colloid and Interface Science*, **220**, 174-176.
10. Gunko, V. M., Zarko, V. I., Leboda R., Chibowski, E. 2001. “Aqueous suspensions of fumed oxides: particle size distribution and zeta potential”, *Advances in Colloidal and Interface Science*, **91**, 1-112.
11. Logan B. E., 1999. *Enviromental Transport Processes*, Wiley, New York.
12. *Fine Particles Technical Bulletin Number 11: Basic Characteristics of Aerosil® Fumed Silica*. 2006. Degussa AG, Essen, Germany.
13. Rumpf, H., 1962. “The strength of granules and agglomerates” 1962 in *Agglomeration*, (Knepper, W. A. ed.), Wiley, New York, pp. 379-418.
14. Tang S.; Ma, Y.; Shiu, C. 2001. “Modeling of mechanical strength of fractal aggregates” *Colloids and Surfaces A: Physical and Engineering Aspects*, **180**, 7-16.
15. Rwei, S. P.; Manas-Zloczower, I. and Feke, D.L. 1990 “Observation of carbon black agglomerate dispersion in simple shear flows”. *Polym. Engng Sci.*, **30**, 701-706.
16. Rwei, S. P.; Manas-Zloczower, I. and Feke, D.L.1991 “Characterization of agglomerate dispersion by erosion in simple shear flows” . *Polym. Engng Sci.*, **31**, 558-562.
17. Crum, L. 1988. “Cavitation microjets as a contributory mechanism for renal disintegration in ESWL”, *J. Urol.* **148**, 1587-1590.
18. McGraw, R. 1997. “Description of aerosol dynamics by the quadrature method of moments”, *Aerosol Science and Technology*, **27**, 255 -265.
19. Buyevich Yu. A.; Kapbsov S. K. 1999. Segregation of a fine suspension in channel flow, *J.Non-Newt. Fluid. Mech.*, **86**, 157-184.